Pseudoreversion of the Catalytic Activity of Y14F by the Additional Substitution(s) of Tyrosine with Phenylalanine in the Hydrogen Bond Network of Δ^5-3-Ketosteroid Isomerase from *Pseudomonas putida* Biotype B

Gildon Choi, Nam-Chul Ha, Min-Sung Kim, Bee-Hak Hong, Byung-Ha Oh, and Kwan Yong Choi*

Division of Molecular and Life Sciences, Pohang University of Science and Technology, Pohang, Kyungbuk, South Korea

Received December 5, 2000; Revised Manuscript Received March 13, 2001

ABSTRACT: Δ^5-3-ketosteroid isomerase (KSI) from *Pseudomonas putida* Biotype B catalyzes the allylic isomerization of Δ^5-3-ketosteroids to their conjugated Δ^4-isomers via a dienolate intermediate. Two electrophilic catalysts, Tyr-14 and Asp-99, are involved in a hydrogen bond network that comprises Asp-99 Oδ2···O of Wat504···Tyr-14 Oη···Tyr-55 Oη···Tyr-30 Oη in the active site of *P. putida* KSI. Even though neither Tyr-30 nor Tyr-55 plays an essential role in catalysis by the KSI, the catalytic activity of Y14F could be increased ca. 26−51-fold by the additional Y30F and/or Y55F mutation in the hydrogen bond network. To identify the structural basis for the pseudoreversion in the KSI, crystal structures of Y14F and Y14F/Y30F/Y55F have been determined at 1.8 and 2.0 Å resolution, respectively. Comparisons of the two structures near the catalytic center indicate that the hydrogen bond between Asp-99 Oδ2 and C3−O of the steroid, which is perturbed by the Y14F mutation, can be partially restored to that in the wild-type enzyme by the additional Y30F/Y55F mutations. The kinetic parameters of the tyrosine mutants with the additional D99N or D99L mutation also support the idea that Asp-99 contributes to catalysis more efficiently in Y14F/Y30F/Y55F than in Y14F. In contrast to the catalytic mechanism of Y14F, the C4 proton of the steroid substrate was found to be transferred to the C6 position in Y14F/Y30F/Y55F with little exchange of the substrate 4β-proton with a solvent deuterium based on the reaction rate in D_2O. Taken together, our findings strongly suggest that the improvement in the catalytic activity of Y14F by the additional Y30F/Y55F mutations is due to the changes in the structural integrity at the catalytic site and the resulting restoration of the proton-transfer mechanism in Y14F/Y30F/Y55F.

Δ^5-3-Ketosteroid isomerase (KSI)[1] catalyzes the allylic isomerization of the 5,6 double bond of Δ^5-3-ketosteroids to the 4,5 position at a rate approaching the diffusion limit by an intramolecular proton transfer (*1*, *2*). The reaction is initiated by the abstraction of a proton from the C4 position of the steroid substrate by Asp-38 to generate a dienol(ate) intermediate (*3*, *4*). The intermediate generated during the enolization step is subsequently reketonized by the transfer of the C4 proton abstracted by Asp-38 from the substrate to the C6 position (*2*). The KSI reaction is not completely stereospecific since both the C-4α and C-4β protons can be abstracted by the catalytic base and transferred to the C6 position (*5*). In the proton-transfer process, Tyr-14 contributes to catalysis by stabilizing the unstable reaction intermediate with a negative charge through the formation of a normal (*4*) or low-barrier hydrogen bond (*6*) with the intermediate. The stabilization enables the unfavorable proton transfer from the C4 to C6 position of the steroid to proceed rapidly in the catalytic reaction by KSI (*7*, *8*). Consistent with the critical roles of Tyr-14 and Asp-38 in catalysis by *Pseudomonas putida* KSI, the k_{cat} values were dramatically decreased by ca. $10^{3.3}$- and $10^{6.2}$-fold for Y14F and D38N, respectively, relative to that for the wild-type (*9*). While the effects of the Y14F and D38N mutations on catalysis are additive in Y14F/D38N of *Comamonas testosteroni* KSI which is completely inactive (*10*), the same mutant of *P. putida* KSI did not exhibit any additive effect since the k_{cat} value is almost similar to that of D40N (*11*).

Asp-99, a recently identified electrophilic catalyst, is also expected to play a critical role in stabilizing the dienolate intermediate (*8*, *12*−*16*). While there is controversy over whether Asp-99 forms a hydrogen bond with the C3−O of the steroid (*12*−*14*) or with Tyr-14 Oη (*16*, *17*), X-ray crystallographic studies combined with kinetic and quantum mechanical calculations (*18*, *19*) strongly support the direct hydrogen bonding of Asp-99 with the C3−O of the steroid (Figure 1). Additive effects on the kinetic parameters of the Y14F and D99A mutations in Y14F/D99A are also consistent with the absence of a hydrogen bond between Tyr-14 and Asp-99 (*20*).

Tyr-14 and Asp-99 are involved in a hydrogen bond network composed of Asp-99 Oδ2···O of Wat-504···Tyr-

† This work was performed by use of the X-ray Facility at Pohang Accelerator Laboratory and was supported by grants from Korea Science and Engineering Foundation and in part by the Brain Korea 21 project.

* To whom correspondence should be addressed. Phone: (82-54) 279-2295. Fax: (82-54) 279-2199. E-mail: kchoi@postech.ac.kr.

[1] Abbreviations: KSI, Δ^5-3-ketosteroid isomerase; WT, wild-type KSI; NMR, nuclear magnetic resonance; 5-AND, 5-androstene-3,17-dione; *d*-equilenin, *d*-1,3,5(10),6,8-estrapentaen-3-ol-17-one; ppm, part per million; SDS−PAGE, sodium dodecyl sulfate−polyacrylamide gel electrophoresis; K_M, Michaelis constant; k_{cat}, first-order rate constant for the reaction of enzyme−substrate complex to yield a product.

10.1021/bi002767+ CCC: $20.00
Published on Web 05/16/2001

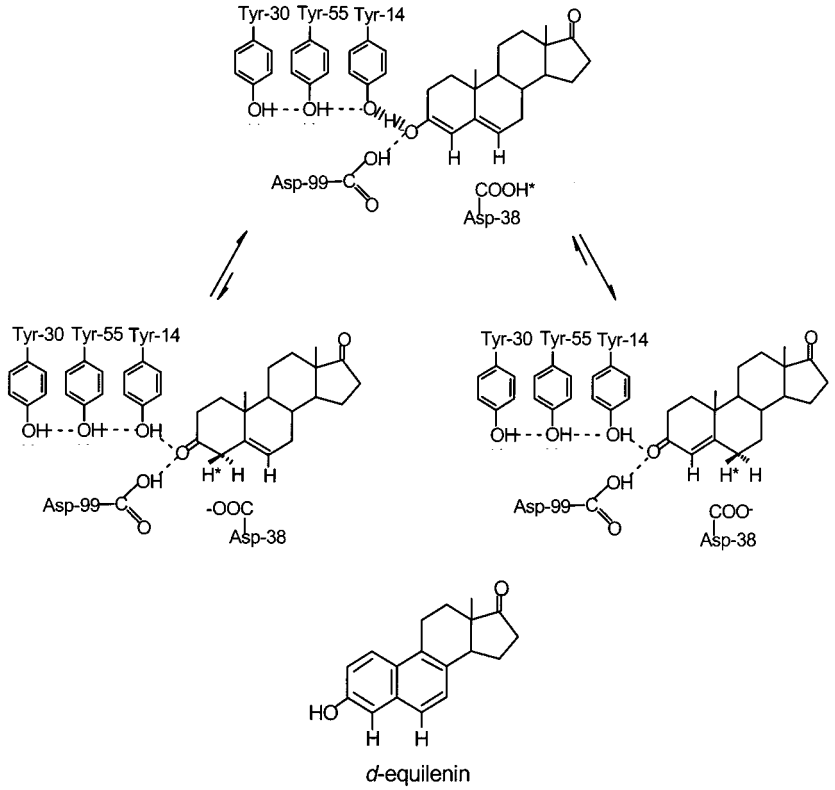

FIGURE 1: Reaction catalyzed by ketosteroid isomerases. 5-androstene-3,17-dione, a substrate of KSI, is converted to a product, 4-androstene-3,17-dione, via the dienolate intermediate. The proton at C-4 is transferred by Asp-38 to the β side of C-6 during the isomerization reaction. Both Tyr-14 and Asp-99 stabilize the intermediate by forming a hydrogen bond with the C3−O of the intermediate. Tyr-14 is hydrogen-bonded to Tyr-55 that is in turn hydrogen bonded to Ty-30 in *P. putida* KSI. Tyr-30 is homologously replaced by a phenylalanine residue in *C. testosteroni* KSI. *d*-Equilenin is an intermediate analogue of KSI.

14 Oη···Tyr-55 Oη···Tyr-30 Oη in the active site of *P. putida* KSI (*13*) (Figure 1) (the residues of *P. putida* KSI are numbered according to those of *C. testosteroni* KSI throughout the text). Tyr-30 is homologously substituted by a phenylalanine residue in *C. testosteroni* KSI (*14*). Wat-504, a water molecule present between Tyr-14 and Asp-99, is replaced by the C3−O of the steroid when the steroid is bound to the enzyme (*13*, *18*). In contrast to the critical roles of Tyr-14 and Asp-99 in catalysis by KSI, neither Tyr-30 nor Tyr-55 is essential for catalysis since the k_{cat} values were decreased only by ca. 1.2- and 5.9-fold for Y30F and Y55F, respectively (*21*). Consistently, the crystal structure of *P. putida KSI* complexed with d-equilenin, an intermediate analogue, has revealed that neither tyrosine forms a hydrogen bond directly with the bound steroid while they locate closely near Tyr-14 (Figure 1).

In *C. testosteroni* KSI, the Y55F mutation also resulted in only a marginal effect on the catalytic power of the KSI (*3*). When introduced into the Y14F mutant, however, the additional Y55F mutation could increase the catalytic activity of Y14F/Y55F by ca. 30-fold relative to that of Y14F (*22*). On the basis of the catalytic mechanism of Y14F in which the intermediate dissociates rapidly from the active site to the solution (*23*), it has been proposed that the increased catalytic activity of Y14F/Y55F may result from the release of the intermediate more rapidly from the active site of the mutant than from Y14F (*22*). While a 2-fold reduction of the binding affinity of Y14F/Y55F for 19-nortestosterone, a product analogue, relative to that of Y14F has been considered to be the supporting evidence for the suggested mechanism (*22*), no further information is available on the detailed mechanism for the pseudoreversion process in the KSI. The pseudoreversion of a mutational effect on catalysis by a second site mutation have also been observed in many other enzymes including triose phosphate isomerase (*24*, *25*), horseradish peroxidase (*26*) and reverse transcriptase from HIV Type-1 (*27*).

In this study, we report the results of our investigation into the catalytic mechanism of Y14F/Y30F/Y55F of *P. putida* KSI that exhibited the catalytic activity ca. 51-fold higher than Y14F. When the Y30F/Y55F mutations were introduced into the Y14F mutant, the side-chain configuration of Phe-14 in the catalytic center was partially restored to the configuration similar to that of the corresponding tyrosine in the wild-type. Together with the structural analysis for the pseudoreversion in *P. putida* KSI, our kinetic and spectroscopic results strongly suggest that the catalytic activity of Y14F/Y30F/Y55F relative to that of Y14F be increased due to the restoration of the proper structural integrity at the catalytic site which results in the optimal interaction of Asp-99 with the steroid in the triple mutant.

MATERIALS AND METHODS

Materials. 5-Androstene-3,17-dione (5-AND) was purchased from Steraloids. The purity of the steroid was checked by thin-layer chromatography and melting point analysis. The steroid compound exhibited a single spot on thin-layer chromatography with 5% ethyl acetate in hexane as a moving phase. In addition, the melting point of the steroid was found to be 133−135 °C. The identity of the steroid was confirmed by kinetic and spectroscopic methods. The molecular weight

of 5-AND was found to be 286.1 when determined by mass spectrometry, which is very close to the calculated molecular weight of the steroid, 286.4. In addition, two kinds of the carbonyl groups were detected at the wavelength of 1740.8 and 1712.3 nm, respectively, in the infrared spectrum of the steroid, which certainly correspond to the stretching vibration of the two carbonyl groups at the C3 and the C17 positions of 5-AND.

D_2O (99.9 atom % D) and CD_3OD (99.8 atom % D) were from Aldrich. All the chemicals for the buffer solution were from Sigma. Superose 12 gel filtration column was from Pharmacia. All the enzymes for DNA manipulation were from Boehringer Mannheim. Synthetic oligonucleotides were obtained from Genotech Inc., Korea. pBluescript SK(−) [pSK(−)] plasmid was from Stratagen. pKK 223-3 plasmid was from Pharmacia.

Oligonucleotide-Directed Mutagenesis of the KSI Gene. To introduce the Y14F/Y30F, the Y14F/Y55F and the Y14F/Y30F/Y55F mutations into the coding region of *P. putida* KSI gene, the pSK(−) plasmid containing the KSI gene with the respective mutation of Y30F, Y55F, and Y30F/Y55F (*21*) was digested with *Eco*RV and *Hin*dIII to isolate the DNA fragment containing the KSI gene with the desired mutation. The isolated DNA fragment was directly subcloned into the same restriction sites of the pKK-KSI plasmid containing the Y14F mutation (*9*). The resulting recombinant plasmids, pKK-Y14F/Y30F, pKK-Y14F/Y55F, and pKK-Y14F/Y30F/Y55F, were used to express the mutant KSI genes in *Escherichia coli* strain BL21(DE3).

The expression vectors for Y14F/Y30F/Y55F/D99N and Y14F/Y30F/Y55F/D99L were constructed as follows; the entire coding region of the KSI gene with the Y14F/Y30F/Y55F mutation was subcloned into the *Eco*RI and *Hin*dIII sites of pSK(−) plasmid to construct pSK-Y14F/Y30F/Y55F. The resulting recombinant plasmid was subsequently utilized to prepare the single-stranded uracil-containing template DNA complementary to the coding strand of the KSI gene with the Y14F/Y30F/Y55F mutation as described previously (*28*). The synthetic oligonucleotides (D99N, 5′-CTG GAT GTC ATC AAT GTG ATG CGC-3′; D99L, 5′-CTG GAT GTC ATC CTT GTG ATG CGC-3′; the underlined nucleotides are the mismatched ones) were synthesized for the additional D99N and D99L mutation into Y14F/Y30F/Y55F, respectively. Clones of the reconbinant plasmids that contain the desired mutations were identified by digestion with *Cla*I. The entire nucleotide sequences of the mutant genes were determined to confirm that no other mutations except the desired ones occurred during the mutagenesis. The *Eco*RI/*Hin*dIII DNA fragments containing the Y14F/Y30F/Y55F/D99N and Y14F/Y30F/Y55F/D99L mutation were subcloned into the same restriction sites of the pKK 223−3 plasmid to construct the recombinant expression plasmids, pKK-Y14F/Y30F/Y55F/D99N and pKK-Y14F/Y30F/Y55F/D99L, respectively.

Overexpression and Purification of Mutant Isomerases. The procedures for overexpression and purification of *P. putida* KSI were carried out as described previously (*9*) with a slight modification. *E. coli* BL21(DE3) cells harboring the recombinant plasmid were grown in a Luria-Bertani medium containing 100 mg of ampicillin/L until the OD_{600} reached 0.5. After the addition of isopropyl-β-D-thiogalatopyranoside to the final concentration of 0.75 mM, the cells were cultured for an additional 18 h at 37 °C. The overexpressed KSI was purified by deoxycholate affinity chromatography as a principal step and finally by Superose 12 gel filtration chromatography. The purified enzymes were homogeneous as judged by single bands on SDS−PAGE. The concentrations of the purified enzymes were determined by the Bradford colorimetric assay method (*29*) and confirmed by the measurement of the band intensity on SDS−PAGE gel by use of an imaging densitometer (Bio-Rad, GS-700) and a software supplied by the manufacturer (Bio-Rad, Molecular Analyst/PC).

Determination of Kinetic Constants, k_{cat} and K_M. The KSI activity was determined at 25 °C in a buffer solution containing 34 mM potassium phosphate, pH 7.0, 2.5 mM EDTA and variable amount of the steroid substrate, 5-AND, by measuring the product of the enzyme spectrophotometrically as described previously (*15*). The final concentration of methanol in the reaction mixture was 3.3 vol %. The reaction was initiated by the addition of the enzyme. Kinetic parameters such as k_{cat} and K_M were obtained by utilizing Lineweaver−Burk reciprocal plots under the assay condition in which the substrate concentrations were 23.3, 34.9, 58.2, 81.5, and 116.4 μM, respectively.

Analyses of the Isomerization Reactions in D_2O. When the isomerization of the steroid substrate 5-AND was conducted in D_2O by Y14F, the rapid decrease of the reaction rate could be observed. To analyze the rate decrease in a quantitative way as described previously (*23*), the absorbance at 248 nm during the reaction were obtained by use of a computer-interfaced UV spectrophotometer (Cary 5E) and the first-order plot of $\ln([S]_o/[S]_t)$ vs time was made; $[S]_o$ is the substrate concentration at time zero and $[S]_t$ is the concentration at any given time. At substrate concentrations well below the K_M, a straight line should be obtained for a perfect pseudo-first-order reaction and any departure from first-order kinetics could be detected by deviations from linearity.

For the isomerization of 5-AND in D_2O, the substrate was dissolved in CD_3OD. All other components of the reaction mixture were initially dissolved in D_2O, lyophilized and redissolved in D_2O to exchange the proton completely with deuterium. The procedures of the activity assay in deuterated solvent were the same as in protonated solvent except that the final volume of the reaction mixture was reduced to 1.0 mL. In addition, the reaction was initiated by adding the substrate finally to the reaction mixture containing the KSI to eliminate nonenzymatic proton exchange of the substrate prior to enzymatic isomerization as described previously (*5*). The concentrations of the substrate used in the reactions were between 6.3 μM and 8.4 μM, which were assessed by complete enzymatic conversion of the substrate to the product whose molar absorptivity is 16 300 M^{-1} cm^{-1}. The enzymes were appropriately diluted to obtain similar absorbance changes during the reaction times.

Steady-State Fluorescence Spectroscopy. The fluorescence emission spectra of the wild-type KSI and its tryptophan mutants (W88Y and W116Y) were obtained to identify the contribution of each tryptophan residue to the total tryptophan fluorescence of *P. putida* KSI. The emission intensity was measured from 300 to 400 nm after the excitation at 295 nm.

Table 1: Kinetic Parameters of the Wild-Type and Its Mutant KSIs[a]

enzyme	k_{cat} (s^{-1})	K_m (μM)	k_{cat}/K_m ($M^{-1}s^{-1}$)	relative k_{cat}	relative k_{cat}/K_m
WT	27 900 ± 300	50.3 ± 1.7	5.5×10^8	1	1
Y14F[b]	11.5 ± 1.5	26.9 ± 3.9	4.3×10^5	$10^{-3.4}$	$10^{-3.1}$
Y30F[c]	17 790 ± 74	55.2 ± 2.0	3.3×10^8	0.64	0.60
Y55F[c]	3510 ± 1.4	23.0 ± 1.0	1.5×10^8	0.13	0.27
D99N[d]	5709 ± 271	36.8 ± 0.7	1.6×10^8	0.27	0.29
D99L[e]	220 ± 8.9	25.8 ± 0.8	8.7×10^6	$10^{-2.1}$	$10^{-1.8}$
Y30F/D99L[c]	40.7 ± 1.4	73.5 ± 11.5	5.5×10^5	$10^{-2.7}$	$10^{-3.0}$
Y14F/Y30F	302 ± 18	78.7 ± 6.5	3.8×10^6	$10^{-1.9}$	$10^{-2.1}$
Y14F/Y55F	360 ± 14	28.7 ± 4.1	1.3×10^7	$10^{-1.9}$	$10^{-1.6}$
Y14F/Y30F/Y55F	587 ± 43	51.3 ± 6.2	1.1×10^7	$10^{-1.7}$	$10^{-1.7}$
Y14F/D99N[e]	0.71 ± 0.05	47.5 ± 1.5[e]	1.5×10^4	$10^{-4.6}$	$10^{-4.6}$
Y14F/D99L[e]	0.67 ± 0.01	98.2 ± 6.9[e]	6.8×10^3	$10^{-4.6}$	$10^{-4.9}$
Y14F/Y30F/Y55F/D99N	1.1 ± 0.2	57.8 ± 4.5	1.9×10^4	$10^{-4.4}$	$10^{-4.5}$
Y14F/Y30F/Y55F/D99L	0.052 ± 0.008	91.8 ± 8.0	5.7×10^2	$10^{-5.7}$	$10^{-6.0}$

[a] The assays were performed in a buffer containing 34 nM potassium phosphate, pH 7.0, 2.5 mM EDTA, and 3.3% methanol. [b] Data from Kim et al. (*9*). [c] Data from Kim et al. (*21*). [d] Data from Kim et al. (*15*). [e] Data from Choi et al. (*19*).

Fluorescence Quenching by Acrylamide. Fluorescence quenching experiments were carried out by adding aliquots of freshly prepared 8 M acrylamide to the protein solution. The excitation of the intrinsic tryptophan fluorophores in KSI was performed at the wavelength of 295 nm and the emission intensity was measured at 337 nm. The fluorescence quenching by acrylamide for the wild-type KSI was analyzed according to the Stern−Volmer equation (*30*):

$$F_o/F = 1 + K_{sv}[Q] = 1 + k_q\tau_o[Q] = 1 + k_q cF_o[Q] \quad (1)$$

where F_o and F are fluorescence intensities in the absence and presence of quencher, respectively, K_{sv} the Stern−Volmer constant for collisional quenching, [Q] the concentration of the quencher, k_q the rate constant for the quenching reaction, τ_o the lifetime of the fluorophore in the absence of quencher, and c is defined as τ_o/F_o. To compensate for the lifetime difference between the wild-type and the mutant KSI, the fluorescence quenching by acrylamide for the mutant KSIs was analyzed by use of the modified Stern−Volmer equation (*30*):

$$F_o(\text{mut})/F = 1 + K'_{sv}[Q'] = 1 + k_q cF_o(\text{wt})[Q'] \quad (2)$$

where F_o(wt) and F_o(mut) are the fluorescence intensity of the wild-type and the mutant KSI, respectively, in the absence of any quencher, K'_{sv} the modified Stern−Volmer constant and [Q′] the effective concentration of the quencher which is equal to $[Q][F_o(\text{mutant})/F_o(\text{wt})]$. In the eq 2, the change in the slope of the plot reflects a proportional change in k_q, which represents the solvent accessibility of the fluorophore.

Crystallization and Structure Determination. Crystallization of Y14F and Y14F/Y30F/Y55F was accomplished by the hanging drop vapor diffusion methods as described previously (*13*, *19*) with a slight modification. KSI (20 mg/mL) was prepared in a buffer containing 40 mM potassium phosphate, pH 7.0, 1 mM EDTA, and 15 mM β-mercaptoethanol, and subsequently 70 μL of this solution was mixed with 2 μL of 10 mM *d*-equilenin in dimethyl sulfoxide. The optimal conditions for the crystallization of the mutant KSIs were screened by changing the concentrations of ammonium acetate and sodium acetate, pH 4.6 from 2.0 to 0.1 M, respectively.

All diffraction data were collected on a DIP2020 area detector with graphite monochromated CuKα X-rays generated by a rotating anode generator (MacScience M18XHF) operated at 90 mA and 50 kV at room temperature. Data reduction, merging, and scaling were carried out with the programs DENZO and SCALEPACK as described previously (*31*). The structures of Y14F and Y14F/Y30F/Y55F were determined by use of the molecular replacement method utilizing the coordinates of the D38N that had been determined previously (*13*). The refinement was carried out with a computer program X-PLOR version 3.851.

RESULTS

Kinetic Analyses. The k_{cat} and K_M values for the purified mutant KSIs were compared with those of the wild-type as presented in Table 1. Among the tyrosine triad, Tyr-14, Tyr-30, and Tyr-55, in the hydrogen bond network at the active site of *P. putida* KSI (Figure 1), only Tyr-14 seems to act as an electrophilic catalyst since the k_{cat} values of Y30F and Y55F were decreased by ca. 1.2- and 5.9-fold relative to that of the wild-type, respectively (*21*), in contrast with that of Y14F which was decreased by 2000-fold. The Y30F and/or the Y55F mutation, however, could exert significant effects on the catalytic activity of *P. putida* KSI when introduced additionally into the Y14F mutant since the k_{cat} values for Y14F/Y30F, Y14F/Y55F, and Y14F/Y30F/Y55F were found to be increased by ca. 26-, 31-, and 51-fold, respectively, relative to that of Y14F (Table 1). In contrast, the catalytic activity of D99L could not be improved by the additional Y30F mutation as judged by a modest decrease in k_{cat} for Y30F/D99L (*21*). It has been shown previously that the catalytic activities between Y14F/D99N and Y14F/D99L are similar to each other while D99N that retains significant hydrogen bonding capability of the residue at position 99 exhibits ca. 26-fold higher k_{cat} than that of D99L (*19*). Interestingly, when the additional Y30F/Y55F mutations were introduced into Y14F/D99N and Y14F/D99L, respectively, the k_{cat} value was found to be ca. 21-fold higher for Y14F/Y30F/Y55F/D99N than for Y14F/Y30F/Y55F/D99L (Table 1).

Isomerization Reactions of 5-AND in D_2O. When the substrate concentration was well below than K_M in the reaction of KSI, the first-order plot of $\ln([S]_o/[S]_t)$ versus

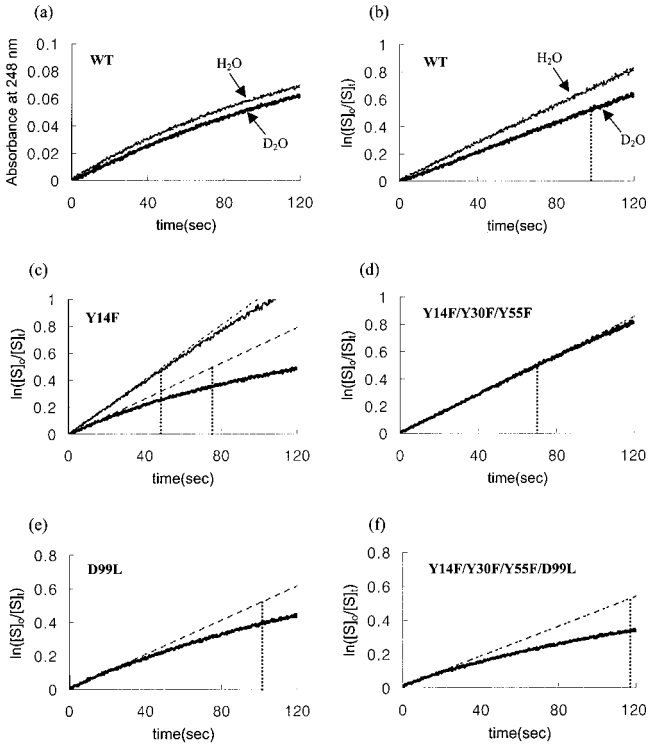

FIGURE 2: First-order plots for the isomerization of 5-androstene-3,17-dione by the wild-type (b), Y14F (c), Y14F/Y30F/Y55F (d), D99L (e), and Y14F/Y30F/Y55F/D99L (f) as a function of time. The absorbance values were monitored at 248 nm during the reaction a and the first-order plots of $\ln([S]_o/[S]_t)$ vs time (b, c, d, e, and f) were constructed from the absorbance values. The thin lines represent the reaction in H_2O and the thick lines the reaction in D_2O. The dotted lines represent the first-order plots extrapolated in the initial phase of the reaction. The vertical line indicates the point where the $\ln([S]_o/[S]_t)$ value obtained from the extrapolation reaches 0.5. The slope of the first-order plot rapidly decreases when the isomerization reaction was carried out in D_2O by Y14F (c). In contrast, the first-order plots of the wild-type (b) and Y14F/Y30F/Y55F (d) were nearly identical to those obtained from the extrapolation.

time in which $[S]_o$ represents the substrate concentration at time zero and $[S]_t$ at any given time, yielded a straight line reflecting a perfect pseudo-first-order reaction (*23*). In the isomerization of 5-AND by the wild-type KSI, straight lines were obtained in the first-order plots for the reactions both in H_2O and D_2O (Figure 2b), implying that the reaction rate can be maintained to be nearly constant during the reaction in both solvents. In contrast, the slope of the first-order plot rapidly decreases when the isomerization reaction was carried out in D_2O by Y14F (Figure 2c). The decrease of the slope in the first-order plot has been attributed to the enzyme catalyzed-exchange of the substrate 4β-proton with a solvent deuterium and the resulting primary kinetic isotope effect at the 4β-position; the C4 proton is abstracted by Asp-38, a catalytic base of KSI, to generate a dienolate intermediate, which is subsequently released from the active site of Y14F and converted preferentially to the substrate rather than to the product in solution (*23*).

The rapid decrease of the reaction rate in the isomerization of the steroid substrate in D_2O by Y14F has been quantitatively measured in the *C. testosteroni* KSI by taking the derivative of the first order plot and subsequently constructing a plot of (k_{cat}/K_M) versus time (*23*). In *P. putida* KSI, however, a very low concentration of the steroid substrate needs to be used in the experiment to maintain the pseudo-first order conditions and consequently the absorbance changes during the reaction were too small to obtain an accurate plot of (k_{cat}/K_M) versus time. Thus, we assessed the amount of the substrate converted actually to the product during the reaction in D_2O and compared it with that estimated from the first-order plot after the extrapolation at the initial phase of the reaction. Upon the extrapolation of the first-order plot up to the point where the $\ln([S]_o/[S]_t)$ value reaches 0.5 (dashed line in Figure 2c), the actual value of $\ln([S]_o/[S]_t)$ for the reaction in D_2O by Y14F (thick line in Figure 2c) was found to be 0.36 ± 0.04, indicating that the rate of the isomerization of the steroid substrate was significantly decreased in D_2O.

Table 2: Crystallographic Data for the Mutant KSIs

	Y14F	Y14F/Y30F/Y55F
resolution (Å)	1.8	2.0
R_{sym} (%)	5.8	8.1
data completeness ($F > 1\sigma$)	93.0	93.1
$R_{standard}$ (%)	20.7	19.0
R_{free} (%)	25.9	26.4
total number of atoms	995	1002
water molecules	39	48
avg *B*-factor (Å^2)	26.87	26.43
rmsd bond length (Å)	0.006	0.013
rmsd bond angle (deg)	1.186	1.572
Ramachandran plot (%)		
most favored region	88.2	86.3
additional allowed region	11.8	13.7
disallowed regions	0	0

The extent of the decrease of the product formation in the reaction catalyzed by each mutant KSI was also estimated by the same method. The actual values of the $\ln([S]_o/[S]_t)$ from the extrapolation were found to be 0.49 ± 0.01, 0.37 ± 0.04, and 0.33 ± 0.03 for Y14F/Y30F/Y55F, D99L, and Y14F/Y30F/Y55F/D99L, respectively. Interestingly, the slope of the first-order plot for the reaction in D_2O by Y14F/Y30F/Y55F were nearly constant (Figure 2d) as found for the reaction by the wild-type, indicating that the substrate 4β-proton exchanges marginally with a solvent deuterium in the reaction by the triple mutant.

Three-Dimensional Structures of Y14F and Y14F/Y30F/Y55F. To identify the structural basis for the pseudoreversion in KSI, the crystal structures of Y14F and Y14F/Y30F/Y55F have been determined at 1.8 and 2.0 Å resolution,[2] respectively. The crystallographic data for the final structures are shown in Table 2. The root-mean-square (rms) differences for all the backbone atoms between the wild-type and Y14F, and between the wild-type and Y14F/Y30F/Y55F were only 0.35 and 0.40 Å, respectively, indicating that the overall structures of the mutant KSIs are very similar to that of the wild-type. However, closer examinations near the catalytic center of Y14F reveal that a notable difference exists in the side-chain configuration of the residue at position 14 between the wild-type and the mutant (Figure 3a). The Cζ carbon of the Phe-14 in Y14F was displaced ca. 1.52 Å away from its original position in the corresponding tyrosine of the wild-type. When the Y30F/Y55F mutations were introduced into Y14F, however, the side-chain configuration of Phe-14 was

[2] The atomic coordinates of Y14F and Y14F/Y30F/Y55F have been deposited with the entry codes, 1EA2 and 1E97, respectively, at the Brookheaven Protein Data Bank.

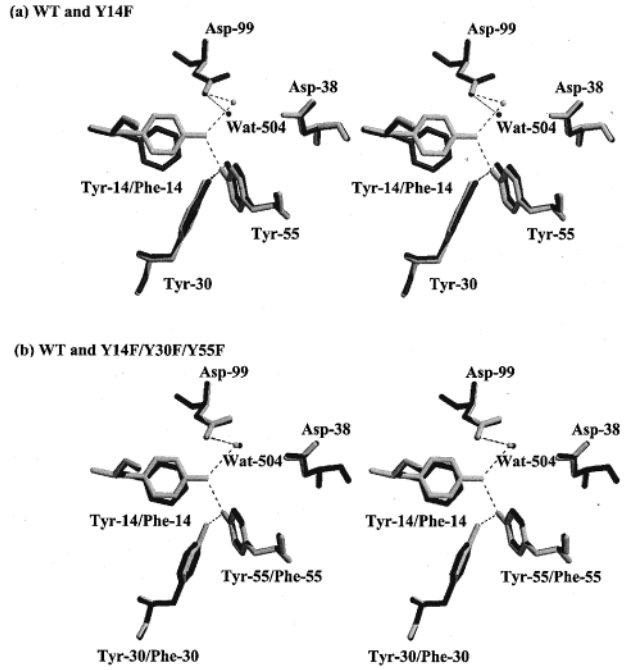

FIGURE 3: Stereoview of the active site residues of the wild-type, Y14F and Y14F/Y30F/Y55F KSI. The corresponding atoms of all the residues were superimpose for (a) wild-type (light gray) and Y14F (dark gray), and (b) wild-type (light gray) and Y14F/Y30F/Y55F (black). The side-chain configuration of Phe-14 in Y14F was significantly altered relative to that of the corresponding tyrosine in the wild-type (a). The side-chain configurations of the three substituted phenylalanines at position 14, 30, and 55 in Y14F/Y30F/Y55F are almost the same as those of the corresponding tyrosines in the wild-type (b). The superposition was performed by use of a computer program Quanta version 2.0 (Molecular Simulations Inc.). The figures were drawn by use of a software, Molscript (*31*).

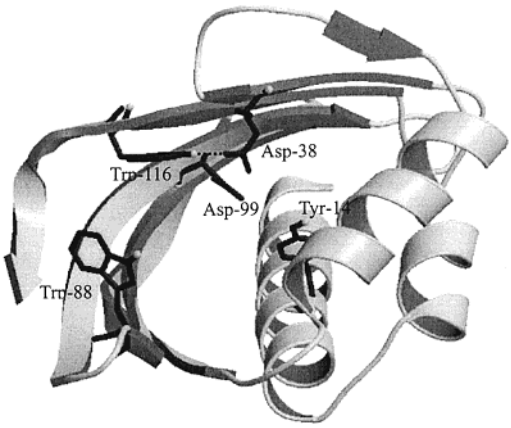

FIGURE 4: Schematic representation of the three-dimensional structure of *P. putida* wild-type KSI. Only one of the two protomers is shown in the figure. Two tryptophan residues (Trp-88 and Trp-116) and three active site residues (Tyr-14, Asp-38, and Asp-99) are shown with the side chains. Trp-88 and Trp-116 are located in the entrance and the inside of the active site. Trp-116 is hydrogen-bonded to Asp-38, a critical catalytic base of KSI. The figure was prepared by use of the program Molscript (*31*).

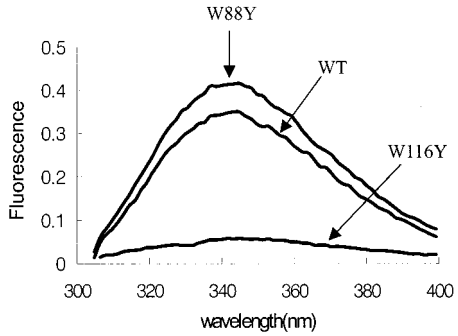

FIGURE 5: Contributions of each tryptophan residue to the fluorescence emission spectrum of the wild-type KSI. Fluorescence spectrum of 5 μM KSI in 40 mM potassium phosphate, pH 7.0 was obtained at 25 °C after the excitation at 295 nm. Comparison of the fluorescence spectrum of W116Y with that of the wild-type strongly indicates that Trp-116 contributes mainly to the total tryptophan fluorescence of *P. putida* KSI.

partially restored to that of the corresponding tyrosine in the wild-type (Figure 3b), resulting in a reduced positional displacement of the Phe-14 Cζ in Y14F/Y30F/Y55F by only ca. 0.69 Å. The superposition of the structure of Y14F/Y30F/Y55F with those of the wild-type and Y14F clearly demonstrates that the change in the side-chain configuration of the residue at position 14 was made by the additional Y30F/Y55F mutations. Interestingly, the side-chain configurations of Asp-99 in Y14F and Y14F/Y30F/Y55F were found to be similar to that of the wild-type without the assistance of a hydrogen bond from Tyr-14 (Figure 3, panels a and b).

Steady-State Fluorescence Spectroscopy of the Wild-Type and Its Tryptophan Mutants. To utilize the tryptophan fluorescence for monitoring the structural changes in the active site of *P. putida* KSI after the mutation made at the hydrogen bond network, it is necessary to determine the contributions of each tryptophan residue to the total tryptophan fluorescence of the KSI. Two tryptophan residues, Trp-88 and Trp-116, are located in the entrance and the inside of the active site of *P. putida* KSI, respectively (Figure 4). Trp-116 is hydrogen-bonded to Asp-38, the critical catalytic base of the KSI. The fluorescence spectrum of the wild-type represented the typical emission of a tryptophan with λ_{max} at 340 nm (Figure 5), consistent with the relatively solvent-accessible environment of the tryptophan residue. The fluorescence intensity of the wild-type KSI was dramatically decreased by the W116Y mutation (Figure 5), suggesting that the tryptophan fluorescence of the wild-type *P. putida* KSI mainly originates from Trp-116. In contrast, the fluorescence intensity of W88Y was more or less increased relative to that of the wild-type (Figure 5), indicating that Trp-88 contributes little to the overall tryptophan fluorescence of *P. putida* KSI.

Acrylamide quenching of the wild-type and its mutant KSIs. Fluorescence quenching by acrylamide is widely used to investigate the microenvironment of the fluorescent groups in proteins (*32*, *33*). The modified Stern−Volmer plots for the fluorescence quenching of the wild-type, Y14F, Y14F/Y30F/Y55F, D99L, and Y14F/Y30F/Y55F/D99L by acrylamide are shown in Figure 6. The slope of the plot reflects the extent of water accessibility of the tryptophan residues in *P. putida* KSI, especially Trp-116 since the tryptophan fluorescence of the KSI mainly originates from the tryptophan residue. The slope of the modified Stern−Volmer plot for the acrylamide-quenching of the wild-type KSI was substantially decreased by the Y14F and the D99L mutations, indicating that the solvent accessibility of the active site of Y14F and D99L near Asp-38 is decreased relative to that of the wild-type. Interestingly, the slope of the plot of Y14F/Y30F/Y55F was significantly increased relative to that of Y14F up to the level of the wild-type, implying that the microenvironment near Asp-38 in Y14F might be partially

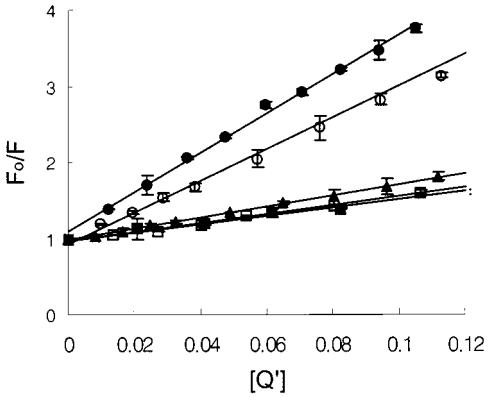

FIGURE 6: Stern-Volmer plots for the acrylamide quenching of the intrinsic tryptophan fluorescence of the wild-type and its mutant KSIs: (●) wild-type KSI, (○) Y14F/Y30F/Y55F, (■) Y14F, (□) D99L, (▲) Y14F/Y30F/Y55F/D99L. Acrylamide was successively added to the 5 μM solution of KSI. In the plots, F_o and F represent the fluorescence intensities in the absence and presence of acrylamide, respectively. [Q′] is the effective concentration of the quencher and is equal to [Q][F_o(mutant)/F_o(wt)]. The slopes of the plots calculated by use of eq 2 are 25.9 ± 1.7, 20.0 ± 0.9, 5.4 ± 0.1, 5.9 ± 0.2, and 7.2 ± 0.4 for the wild-type, Y14F/Y30F/Y55F, Y16F, D99L, and Y14F/Y30F/Y55F/D99L, respectively.

restored by introducing the additional Y30F/Y55F mutations into the Y14F mutant.

DISCUSSION

When Tyr-14, the electrophilic or general acidic catalyst of KSI, was substituted with phenylalanine, the k_{cat} value was substantially decreased by ca. 2000-fold for Y14F relative to that for the wild-type *P. putida* KSI. Significant portions of the activity decrease by the Y14F mutation should be attributed to the destabilization of the dienolate intermediate and its related transition state(s) by the loss of a hydrogen bond between Tyr-14 and the steroid. In addition, the absence of both of the proton peaks assigned to Tyr-14 OH and Asp-99 COOH, respectively, in the ^{1}H NMR spectrum of Y14F/D38N complexed with *d*-equilenin (*18*) suggests that the Y14F mutation not only abolishes the hydrogen bond between Tyr-14 and the steroid but also perturbs the proper interaction of Asp-99 with the steroid. The catalytic activity of Y14F/D99N was found to be similar to that of Y14F/D99L while D99N that retains some hydrogen bonding capability at position 99 exhibited a k_{cat} ca. 26-fold higher than that of D99L (*19*), which is consistent with the results obtained by NMR spectroscopy for Y14F.

Although the crystal structure and the ^{1}H NMR spectrum of Y14F/Y30F/Y55F/D38N complexed with *d*-equilenin can help to identify the formation of an enzyme-steroid complex in the mutant similar to that in the wild-type, we could not obtain a sufficient amount of the mutant needed for the experiment because of its very low expression level in our expression system. However, the kinetic parameters of the tyrosine mutants containing the additional D99N or D99L mutation could support the idea that Asp-99 contributes to catalysis more efficiently in Y14F/Y30F/Y55F than in Y14F; while the catalytic activities between Y14F/D99N and Y14F/D99L are similar to each other, the additional Y30F/Y55F mutations rendered the catalytic activity of Y14F/Y30F/Y55F/D99N ca. 21-fold higher than that of Y14F/Y30F/Y55F/D99L (Table 1). These kinetic results strongly suggest that the perturbed interaction of Asp-99 with the steroid by the Y14F mutation can be partially restored to that in the wild-type by the additional Y30F/Y55F mutations.

The crystal structure of Y14F without the steroid has revealed that the side-chain configuration of Phe-14 was altered significantly relative to that of the corresponding tyrosine in the wild-type (Figure 3a). By introducing the additional Y30F/Y55F mutations into the Y14F mutant, the side-chain configuration of Phe-14 in Y14F/Y30F/Y55F was converted to be similar to that of the corresponding tyrosine in the wild-type (Figure 3b). The acrylamide quenching of the intrinsic tryptophan fluorescence of the wild-type and its mutant KSIs (Figure 6) also suggests that the introduction of the Y30F/Y55F mutations into the Y14F mutant causes a structural change in the active site. The quenching efficiency of Y14F/Y30F/Y55F by acrylamide, which is increased up to the level of the wild-type, indicates that the microenvironment near Trp-116 in the active site of the mutant is very similar to that of the wild-type. The changes in the microenvironment near Trp-116 may be closely related to catalysis by *P. putida* KSI since the tryptophan residue is hydrogen-bonded to Asp-38, a critical catalytic base of the KSI. Thus, together with the crystal structure of Y14F/Y30F/Y55F, the quenching efficiency of the mutant by acrylamide support the idea that the pseudoreversion of the catalytic activity of Y14F by the additional Y30F/Y55F mutations is due to the partial restoration of the proper structural integrity at the catalytic site.

It was previously reported that the pseudo first-order rate constant for the isomerization in D_2O by *C. testosteroni* Y14F KSI rapidly decreases as the reaction proceeds and was interpreted as an evidence for the dissociation of the intermediate from the active site of the mutant, which is partially rate limiting (*23*). The released intermediate is subsequently reketonized to regenerate the substrate or converted to the product. On the basis of the catalytic mechanism of *C. testosteroni* Y14F KSI, the catalytic activity of *C. testosteroni* Y14F/Y55F KSI ca. 30-fold higher than that of Y14F was proposed to be due to the more rapid release of the intermediate from the active site in the presence of the additional Y55F mutation (*22*). This proposal can be controversial since the rate-limiting step in the nonenzymatic isomerization of 5-AND to 4-AND, the reaction product, is protonation of the dienolate intermediate at C6 position (*34*, *35*). On the basis of this result, the increased catalytic activity of *C. testosteroni* Y14F/Y55F KSI might not be due to an increased rate of dissociation of the intermediate from the active site. The reaction rate of *P. putida* Y14F/Y30F/Y55F in D_2O was found to be nearly constant, indicating that the C4 proton abstracted by Asp-38, a catalytic base of KSI, is transferred to the C6 position inside the active site as in the reaction by the wild-type enzyme. The 51-fold increased catalytic activity of Y14F/Y30F/Y55F relative to that of Y14F could be attributed to the restoration of the proton-transfer process in the triple mutant as that in the wild-type KSI. If the catalytic mechanism of *C. testosteroni* Y14F/Y55F KSI is similar to that of *P. putida* Y14F/Y30F/Y55F KSI, the pseudoreversion of the catalytic activity of Y14F by the additional Y55F mutation in *C. testosteroni* is also due to the partial restoration of the proton-transfer process by the proper structural integrity at the catalytic site rather

than the increased rate of dissociation of the intermediate from the active site.

In conclusion, we have found that the catalytic activity of Y14F/Y30F/Y55F increased by ca. 51-fold compared to that of Y14F KSI from *P. putida*. The structural characteristics around the active site of the triple mutant was found to be similar to that of the wild-type enzyme as demonstrated by X-ray crystallography and fluorescence spectroscopy. The pseudoreversion of the catalytic activity of Y14F KSI achieved by the additional substitution of tyrosines with phenylalanines near Tyr-14 seems to originate from the partial restoration of the active site leading to the proton-transfer process in Y14F/Y30F/Y55F as that in the wild-type KSI. Determination of rate constants of such element reactions as the enolization and reketonization steps in the tyrosine mutants will contribute to a better understanding for the pseudoreversion of the catalytic activity of Y14F KSI.

REFERENCES

1. Schwab, J. M., and Henderson, B. S. (1990) *Chem. Rev. 90*, 1203−1245.
2. Pollack, R. M., Bounds, P. L., and Bevins, C. L. (1989) In *The chemistry of enones* (Patai, S., and Rappoport, Z., Eds.) John Wiley and Sons Ltd., New York.
3. Kuliopulos, A., Mildvan, A. S., Shortle, D., and Talaray, P. (1989) *Biochemistry 28*, 149−159.
4. Petrounia, I. P., Blotny, G., and Pollack, R. M. (2000) *Biochemistry 39*, 110−116.
5. Zawrotny, M. E., Hawkinson, D. C., Blotny, G., and Pollack, R. M. (1996) *Biochemistry 35*, 6438−6442.
6. Zhao, Q., Abeygunawardana, C., Talalay, P., and Mildvan, A. S. (1996) *Proc. Natl. Acad. Sci. U.S.A. 93*, 8220−8224.
7. Gerlt, J. A., and Gassman, P. G. (1993) *J. Am. Chem. Soc. 115*, 11552−11568.
8. Kim, K. S., Oh, K. S., and Lee, J. Y. (2000) *Proc. Natl. Acad. Sci. U.S.A. 97*, 6373−6378.
9. Kim, S. W., and Choi, K. Y. (1995) *J. Bacteriol. 177*, 2602−2605.
10. Kuliopulos, A., Talalay, P., Mildvan, A. S. (1990) *Biochemistry 29*, 10271−10280.
11. Kim, S. W., and Choi, K. Y. (1995) *Mol. Cell. 5*, 354−358.
12. Wu, Z. R., Ebrahimian, S., Zawrotny, M. E., Thornburg, L. D., Perez-Alvarado, G. C., Brothers, P., Pollack, R. M., and Summers. M. F. (1997) *Science 276*, 415−418.
13. Kim, S. W., Cha, S.-S., Cho, H.-S., Kim, J.-S., Ha, N.-C., Cho, M.-J., Joo, S., Kim, K.-K., Choi, K. Y., and Oh, B.-H. (1997) *Biochemistry 36*, 14030−14036.
14. Cho, H. S., Choi, G., Choi, K. Y., and Oh, B. H. (1998) *Biochemistry 37*, 8325−8330.
15. Kim, S. W., Joo, S., Choi, G., Cho, H.-S., Oh, B.-H., and Choi, K. Y. (1997) *J. Bacteriol. 179*, 7742−7747.
16. Zhao, Q., Abeygunawardana, C., Gittis, A. G., and Mildvan, A. S. (1997) *Biochemistry 36*, 14616−14626.
17. Massiah, M. A., Abeygunawardana, C., Gittis, A. G., and Mildvan, A. S. (1998) *Biochemistry 37*, 14701−14712.
18. Cho, H., −S., Ha, N., −C., Choi, G., Kim, H.-J., Lee, D., Oh, K., S., Kim, K., S., Lee, W., Choi, K. W., and Oh, B.-H. (1999) *J. Biol. Chem. 274*, 32863−32868.
19. Choi, G., Ha, N., −C., Kim, S. W., Kim, D.-H., Park, S., Oh, B.-H., and Choi, K. Y. (2000) *Biochemistry 39*, 903−909.
20. Pollack, R. M., Thornburg, L. D., Wu, Z. R., and Summers, M. F. (1999) *Arch. Biochem. Biophys. 370*, 9−15.
21. Kim, D. H., Jang, D. S., Nam, G. H., Choi, G., Kim, J. S., Joo, S., Oh, B. H., and Choi, K. Y. (2000) *Biochemistry 39*, 4581−4589.
22. Li, Y.-K., Kuliopulos, A., Mildvan, A. S., and Talaray, P. (1993) *Biochemistry 32*, 1816−1824.
23. Xue, L., Talaray, P., and Mildvan, A. S. (1991) *Biochemistry 30*, 10858−10865.
24. Komives, E. A., Lougheed, J. C., Liu, K., Sugio. S., Zhang, Z., Petsko, G. A., and Ringe, D. (1995) *Biochemistry 34*, 13612−12621.
25. Komives, E. A., Lougheed, J. C., Zhang, Z., Sugio. S., Narayana, N., Xuong, N. H., Petsko, G. A., and Ringe, D. (1996) *Biochemistry 35*, 15474−15484
26. Savenkova, M. I., Newmyer, S. L., and Ortiz de Montellano, P. R. (1996) *J. Biol. Chem. 271*, 24598−24603.
27. Harris, D., Yadav, P. N., and Pandey, V. N. (1998) *Biochemistry 37*, 9630−9640.
28. Kunkel, T. A. (1985) *Proc. Natl. Acad. Sci. U.S.A. 82*, 488−492.
29. Bradford, M. M. (1976) *Anal. Biochem. 72*, 248−254.
30. Li, M., Cornea, R. L., Autry, J. M., Jones, L. R., and Thomas, D. D. (1998) *Biochemistry 37*, 7869−7877.
31. Otwinowski, Z. (1993) in *Proceedings of the CCP4 Study Weekend* (Sawyer, L., et al., Eds.) pp 56−62, SERC Daresbury Laboratory, Warrington, U.K.
32. Wang, Q., Matsushita, K., de Foresta, B., le Marie, M., Kaback, H. R. (1997) *Biochemistry 36*, 14120−14127.
33. Szittner, J. L. R., and Meighen, E. A. (1998) *Biochemistry 37*, 16130−16138.
34. Zeng, B. and Pollack, R. M. (1991) *J. Am. Chem. Soc. 113*, 3838−3842.
35. Hawkinson, D. C., Eames, T. C. M., and Pollack, R. M. (1991) *Biochemistry 30*, 10849−10858.

BI002767+